ACS APPLIED MATERIALS & INTERFACES

Research Article

www.acsami.org

Uniform Growth of High-Quality Oxide Thin Films on Graphene Using a CdSe Quantum Dot Array Seeding Layer

Yong-Tae Kim,[†,∥] Seoung-Ki Lee,[‡,∥] Kwang-Seop Kim,[§] Yong Ho Kim,[†,⊥] Jong-Hyun Ahn,*[,‡] and Young-Uk Kwon*[,†,⊥]

[†]SKKU Advanced Institute of Nanotechnology (SAINT), Sungkyunkwan University, Suwon 440-746, Korea

[‡]School of Electrical and Electronic Engineering, Yonsei University, Seoul 120-749, Korea

[§]Department of Nano Mechanics, Nano Convergence Mechanical Systems Research Division, Korea Institute of Machinery & Materials (KIMM), Daejeon 305-343, Korea

[⊥]Department of Chemistry, BK-21 School of Chemical Materials Sciences, Sungkyunkwan University, Suwon 440-746, Korea

Supporting Information

ABSTRACT: Graphene displays outstanding properties as an electrode and a semiconducting channel material for transistors; however, the weak interfacial bond between graphene and an inorganic oxide material-based insulator presents a major constraint on these applications. Here, we report a new approach to improving the interface between the two materials using a CdSe quantum dot (QD)-based seeding layer in an inorganic material−graphene junction. CdSe QDs were electrochemically grown on graphene without degrading the properties of the graphene layer. The graphene structure was then used as the electrode in an oxide semiconductor by depositing a zinc oxide thin film onto the graphene coated with a QD seed layer (QD/G). The zinc oxide film adhered strongly to the graphene layer and provided a low contact resistance. A high-k dielectric layer in the form of an HfO_2 film, which is an essential element in the fabrication of high-performance graphene-based field effect transistors, was also uniformly formed on the QD/G sheet using atomic layer deposition. The resulting transistors provided a relatively good performance, yielding hole and electron mobilities of 2600 and 2000 $cm^2/V{\cdot}s$.

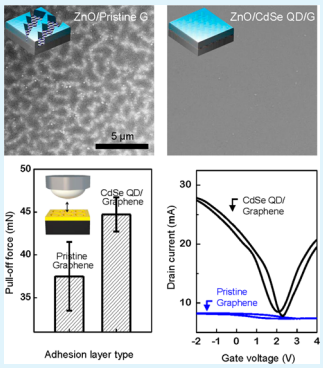

KEYWORDS: *graphene, CdSe quantum dot, contact resistance, seeding layer, oxide thin film*

INTRODUCTION

Graphene has attracted significant attention for its potential utility as a transparent electrode and a semiconducting channel in a variety of electronic devices such as light-emitting diodes (LEDs),[1−3] thin film transistors (TFTs),[4−6] organic photovoltaic (OPV) devices,[7−9] and dye-sensitized solar cells (DSSCs).[10−12] Graphene can form excellent interface contacts with active organic electronic materials through strong $\pi-\pi$ interactions between them. As a result, graphene-based organic devices with high performances have been demonstrated.[13−15] By contrast, the integration of graphene electrodes or channels with inorganic materials such as oxide semiconductors and dielectric materials faces significant challenges. Such graphene/inorganic hybrid systems are deemed to be very useful for practical electronic and energy applications, and much effort has been applied toward improving the interface properties.[16,17] One of the most significant hurdles involved in combining graphene with conventional inorganic materials arises from the poor interfacial interaction between the two dissimilar types of materials. The metal−oxygen bonds in oxide semiconductors and oxide dielectric materials have strong ionic characters, making the bonds polar and nondirectional. On the contrary, the carbon atoms in graphene form nonpolar and strongly directional covalent bonds. Generally, bond formation between such contrasting materials is very unfavorable. If ever formed, such bonds would result in disruption of the inherent properties of either or both of the bonding materials.

Some recent studies have addressed these issues by exploring the surface functionalization of graphene sheets. Two general approaches to the functionalizing graphene sheets have been tested. One approach involves using oxygen plasma treatment to form oxide defects that provide nucleation sites for the growth of inorganic materials,[1,18] and the other involves depositing perylene-based monolayers onto the graphene surfaces.[19] These methods have drawbacks, however, such as reduced electrical conductivity in the graphene due to the generated defects and an increase in the contact resistance due to the insertion of an insulating organic layer, respectively. Recently, a Y_2O_3 monolayer was formed on graphene to demonstrate that a dielectric layer could be grown directly on a graphene layer.[20,21] Whether this method can be applied to semiconductor oxides with chemical characteristics that differ from those of Y_2O_3 remains to be seen.

Received: May 12, 2014
Accepted: July 24, 2014
Published: July 24, 2014

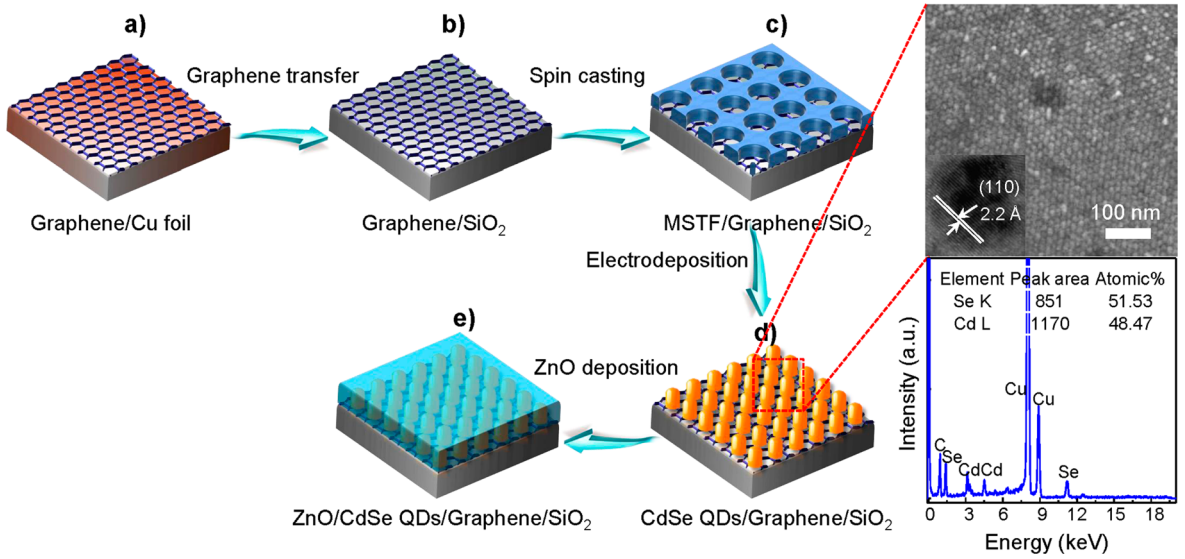

Figure 1. Schematic drawing of the procedure to form ZnO thin film on graphene by using a CdSe QDs seeding layer: The procedure involves (a) the growth of graphene on a Cu foil, (b) transfer of the graphene sheet on a SiO_2/Si substrate by using a PMMA layer as a sample handle, (c) synthesis of a MSTF on the graphene on SiO_2/Si, (d) electrodeposition of CdSe into the pores of the MSTF template followed by the removal of MSTF (In focus images, the SEM image of QD/G shows an array structure of the CdSe QDs on the graphene. The HRTEM image of a CdSe QD in the inset figure shows that the (110) planes of CdSe are oriented perpendicular to the graphene substrate. The EDX spectrum shows Cd and Se peaks with close to 1:1 atomic ratio. The Cu peaks are from the Cu-grid for the TEM measurement.), and (e) growth of ZnO film by sputtering.

Here, we report a novel method of using an inorganic seeding layer to produce metal oxide−graphene junctions. Based on the above-mentioned considerations on the nature of bonding characters of involved materials, we conjectured that the formation of such a junction would require a seeding layer composed of an "adhesive material" with intermediate bonding characters. Metal chalcogenides would be an ideal candidate for such a purpose for their intermediate bonding characters between graphene and metal oxides. Also they may be able to form junctions between oxide semiconductors and graphene with good transport properties. We, therefore, propose that CdSe quantum dot (QD) arrays formed on graphene, we have reported previously,[22,23] can be used as the adhesive layer in growing metal oxide thin films to be grown on top of it. The seeding layer we studied was composed of a CdSe QD array with a few nanometers in thickness that had been electrochemically grown on graphene. The process by which CdSe QDs form on graphene (QD/G) has been shown not to induce the formation of defects on the graphene surface. A zinc oxide (ZnO) thin film, which is a representative oxide semiconductor, was deposited on the CdSe QD-coated graphene (ZnO/QD/G) by sputtering. The ZnO layer displayed better adhesion properties and contact resistance compared to ZnO film deposited on a pristine graphene layer (ZnO/G). The contact resistance depended strongly on the thickness of the CdSe QD seeding layer. A high-quality high-k dielectric oxide layer, HfO_2, was formed on the CdSe QD on graphene (HfO_2/QD/G) by atomic layer deposition (ALD). The uniform HfO_2 layer displayed outstanding dielectric properties in graphene transistors.

EXPERIMENTAL SECTION

Device Fabrication. Graphene films were synthesized via chemical vapor deposition (CVD) on 25 μm thick Cu foils, which had been placed in a quartz tube under an argon atmosphere.[24] The temperature was increased to 1000 °C under a H_2 flow (10 sccm), and a reaction gas mixture of CH_4 (15 sccm) and H_2 (10 sccm) was subsequently introduced. After growth, the temperature was reduced at a rate of 10 °C/s. The graphene on the back side of the device was removed by O_2 plasma etching after protecting the front side with a PMMA coating. Graphene films were transferred to a 300 nm SiO_2/Si substrate after the Cu foil had been etched in an ammonium persulfate solution. A CdSe QD array was formed on graphene by electrochemical deposition on a graphene/SiO_2/Si substrate whose surface was coated with a mesoporous silica thin film (MSTF) to be used as a nanoporous template.[22,23] A precursor solution of MSTF, prepared by dissolving tetraethoxyorthosilicate (TEOS, 99.999%) and a pluronictriblock copolymer (F-127) in a mixed solution containing dilute aqueous HCl and absolute ethanol to a composition ratio of TEOS:F-127:HCl:H_2O:EtOH = 1:6.60 × 10^{-3}:6.66 × 10^{-3}:4.62:22.6 (molar ratio), was spin-coated onto a graphene/SiO_2/Si substrate, aged at 80 °C, and calcined at 400 °C to be used as a nanoporous template. The template included regularly ordered pores with hexagonal symmetry. The pore size was 8 nm and the wall thickness was 4 nm.[25] A MSTF-coated graphene structure was used as the working electrode. A corner of the MSTF on the graphene/SiO_2/Si was etched away to reveal the graphene surface and to enable electrical contact with a wire for the subsequent electrochemical deposition. A Ag/AgCl reference with a Pt counter electrode was used in a three-electrode cell with an aqueous electrolyte solution (0.3 M $CdSO_4$, 0.003 M SeO_2). CdSe was deposited under a constant potential of −0.7 V by using a potentiostat (Ivium compactstat) at 50 °C.[26] After deposition, the MSTF template was removed by dissolving in an aqueous 0.2 wt % HF solution.

ZnO Formation. A 100 nm thick ZnO film was deposited by RF magnetron sputtering system (SPS series (ULTECH)) at room temperature using a high-purity Zn target (4 in., 99.99%, LTS Chemical Inc.). The ratio of the Ar/O_2 sputtering gases was 40/5 sccm at an RF power density of 150 W. The rectangular shape of the ZnO pattern was obtained using a typical lift-off method.

HfO_2 Formation. A 20 nm thick HfO_2 film layer was deposited using a PE-ALD system (Quros Co.; PLUS-200). Tetrakis-(dimethylamino)hafnium (TDMAH) and O_2 were used as the Hf and O precursors, respectively. The flows of the reactant gas (O_2) and purging gas (Ar) were controlled using a mass flow controller. The flow of the O_2 was 25 sccm, and the plasma power was 300 W. The growth temperature was 250 °C, and the growth rates (1.2 Å/cycle) were determined by ellipsometry.

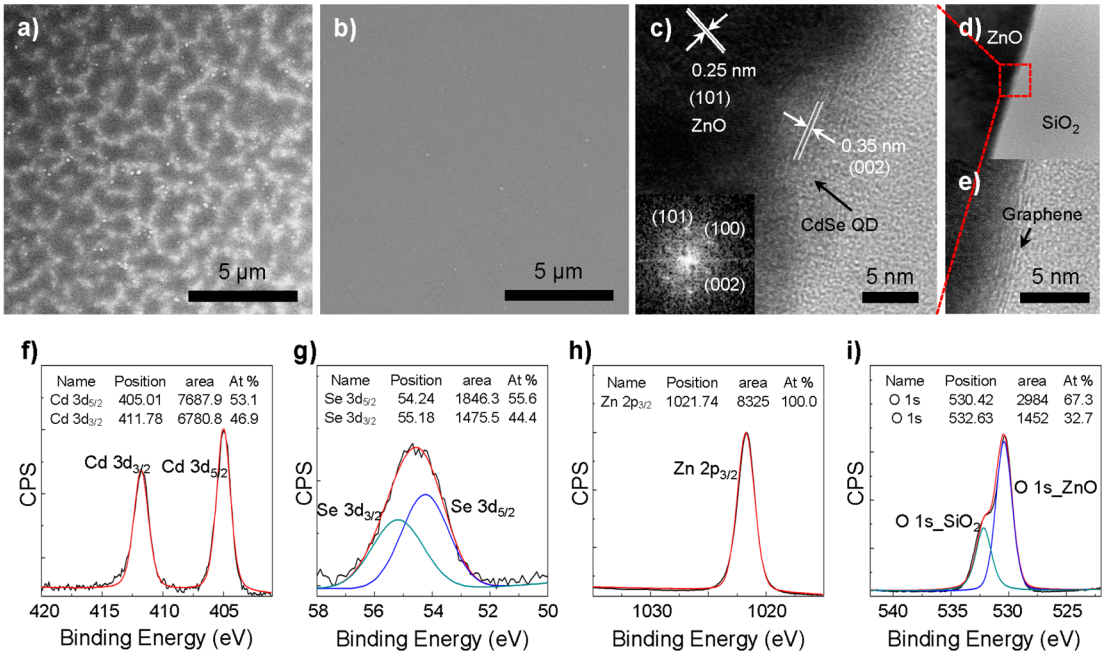

Figure 2. Electron microscopy images and XPS spectra of ZnO thin films on graphene substrates by using a CdSe QDs seeding layer. SEM images ZnO thin films on a pristine graphene (a) and on a QD/G (b). (c–e) Cross-section TEM images of ZnO film grown on QD/G substrate. (c and e) Enlarged images of part d to show the epitaxially grown CdSe QDs on pristine graphene sheet (c) and the presence of trilayer graphene substrate (e). The inset FFT evidence that the ZnO film is imaged along the [1 0 1] zone axis (c). (f–i) XPS spectra of Se 3d, Cd 3d, O 1s, and Zn 2p.

Characterization. Field-emission scanning electron microscopy (SEM; JEOL JSM-7100F, 5–10 kV), high-resolution transmission electron microscopy (TEM; JEOL JEM-3010, 300 kV), and atomic force microscopy (AFM, Park systems XE-100; noncontact mode) were used to characterize the morphologies of the samples. Raman spectra were recorded using a Renishaw RM 1000-invia system with 514 nm excitation and a notch filter 50 cm^{-1} in width. The spectral resolution was 0.2 cm^{-1}. X-ray photoemission spectroscopy (XPS) was performed using the Kα surface analysis system (Thermo VG, U.K.). XPS measurements were carried out using Al–Kα X-ray line (1486.6 eV), the pass energy of survey scan has measured with 100 eV, the energy scale of the spectrometer has been calibrated with C 1s (285 eV), and the base pressure in the XPS analysis chamber was 2.9×10^{-9} mb.

RESULTS AND DISCUSSION

The processes to form QD/G and ZnO/QD/G are schematically outlined in Figure 1. Graphene was synthesized by a chemical vapor deposition (CVD) process on a Cu foil, which is known to produce mostly monolayer (>98%) graphene. After growth, the graphene (1.5×1.5 cm^2) was transferred onto a 300 nm thick SiO_2/Si substrate (2×2 cm^2) using a poly(methyl methacrylate) (PMMA) overcoating method, as reported.[24] This process was repeated to form trilayer graphene films that ensured a sufficient and uniform current when used as an electrode in most of the present study. In order to see the effect of the stacking of graphene layers, monolayer graphene was also used in some cases. A MSTF was formed on the graphene layer to provide a nanoporous template, as reported previously.[22,23] This template consisted of regularly ordered vertical pores with hexagonal symmetry when viewed from the top. The pore size was 8 nm and the wall thickness was 4 nm.[25] CdSe QDs were formed inside the pores by electrochemical deposition in an electrolyte solution composed of $CdSO_4$ and SeO_2 in water. By controlling the deposition time, the thickness of the CdSe QDs could be controllably tuned between 2 and 20 nm. After deposition, the MSTF template was removed with dilute HF. The resulting CdSe QDs form hexagonal arrays which cover the entire graphene surface except the region previously covered by the template wall when the QD thickness is 10 nm or larger (focus of Figure 1d). The composition CdSe QDs was verified to be close to stoichiometric by EDS (Cd/Se = 1.06) and XPS (1.17, Figure 2f and g). In the Raman spectrum of QD/G, the D-peak is absent (Supporting Information Figure S1), suggesting that the procedure to fabricate QD/G does not produce any significant level of damage to graphene. The presence of CdSe QDs does not affect the transmittance properties of graphene significantly (Supporting Information Figure S2). The properties of the modified surfaces were verified by contact angle measurements (Supporting Information Figure S3). Finally, a ZnO thin film was deposited on the QD/G by radio frequency (RF) magnetron sputtering.

The field emission scanning electron microscopy (FE-SEM) images in Figure 2a and b show ZnO thin films with a few nanometers thick grown on the pristine graphene and QD/G substrates, respectively. The ZnO film grown directly on the pristine graphene showed nonuniform surface property because of the aforementioned incompatible bond between ZnO and graphene. In contrast, the ZnO film grown on the QD/G sheet was uniform and displayed a smooth surface morphology (Figure 2b). QD arrays that are chemically compatible with ZnO can activate the nucleation of ZnO and, as a result, lead to the formation of a uniform ZnO film. The cross-sectional high-resolution transmission electron microscopy (HRTEM) images of a ZnO/QD/G sample shown in Figure 2c–e show the graphene layers and the lattice fringes of the CdSe QD and the ZnO film. The lattice fringes of the QDs, which were identified as corresponding to the (002) planes of the wurtzite lattice, were parallel to the graphene layer, suggestive of coordination bonds between the π-orbitals of carbon atoms and the d-

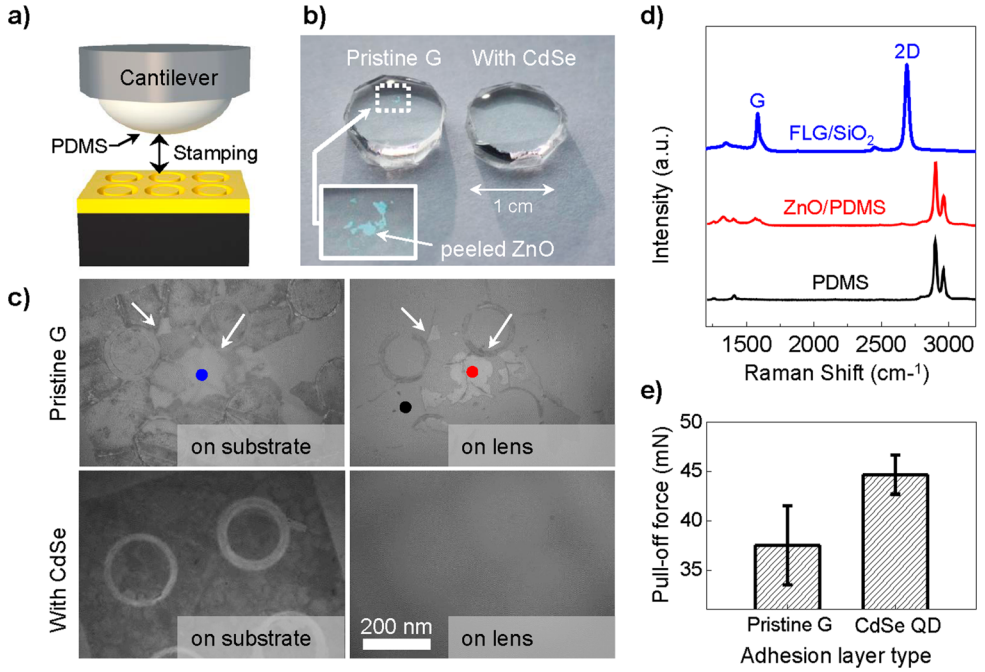

Figure 3. (a) Schematic drawing of the instrument for adhesion test, (b and c) optical microscopy images of PDMS lens and substrate after the adhesion measurement, (d) Raman spectra of various places after the adhesion test on a ZnO/G sample, and (e) comparison of the pull-off forces of ZnO thin films on pristine graphene and QD/G.

orbitals of Cd(II) ions in the CdSe QDs,[23] similar to the suggested interactions between CdSe QDs and carbon nanotubes (CNTs).[27,28] In order to probe the nature of bonding at the ZnO-CdSe QD interface, we took the X-ray photoelectron spectroscopy (XPS) depth profile (Figure 2f–i). The Zn 2p peak is gradually shifted from that of ZnO to that of Zn(II) ion bonded to O(2−) and Se(2−) (Supporting Information Figure S4), clearly demonstrating that the ZnO film is grown on CdSe QDs through chemical bonds.

The adhesion properties between the graphene substrate and the ZnO thin film were examined using a home-built microtribometer, as shown in Figure 3a. A polydimethylsiloxane (PDMS) lens with a radius of curvature of 10.3 mm was attached to the end of the cantilever. The sample was pressed against the lens until the load reached a predetermined maximum value (300 mN), and the contact was maintained for a dwell time (60 s). The sample was then lowered at a constant speed (10 μm/s). The experimental procedure and the measurement parameters are described in detail in Supporting Information Table S1. Figure 3b shows optical images of the lenses after the adhesion tests on ZnO/G and ZnO/QD/G samples. As shown in the lens in the left-hand side of Figure 3b, the test on ZnO/G left ZnO flakes on the lens, whereas ZnO/QD/G did not leave any residue. Magnified optical images of the surfaces of the lenses and the samples are shown in Figure 3c (The circular patterns of the ZnO films had been formed during a sputtering process using masks for the resistance measurements and were not directly related to the adhesion tests.). As shown in the images, the ZnO film on pristine G was heavily damaged, and the surface of the lens was contaminated with ZnO flakes that had peeled off from the sample. The damage to the ZnO film was further verified by inspection of the Raman spectra collected at various locations on the sample and lens surfaces (Figure 3d). Each Raman spectrum in Figure 3d is taken on the spot of corresponding color in Figure 3c. The presence of ZnO on the lens (red spot) was verified by the characteristic peaks of ZnO in the Raman spectrum. In some regions of the sample (i.e., blue spot), the G- and 2D-bands at 1588 and 2700 cm^{-1}, respectively, of graphene with an intensity ratio of 2D/G = 2.3 were observed indicating that ZnO had been peeled off from the graphene substrate. The same spectrum also revealed the D-peak that had not been observed in the Raman spectra of graphene prior to the ZnO film growth (Supporting Information Figure S1). The ZnO film can form strong bonds on the grain boundaries and defects but not on the defect-free regions of the basal plain of CVD graphene, making the binding between the ZnO film and graphene in ZnO/G inhomogeneous. As a result, the adhesion test induces detachment of ZnO from the underlying graphene in some regions while other regions of the sample maintained ZnO. Because of the unevenly distributed strong bonds, the peeling off of ZnO from graphene is likely to induce damages on the exposed graphene (Supporting Information Figure S5). Consequently, both the graphene and the ZnO film had been damaged during the adhesion test. By contrast, the ZnO film on the QD/G surface remained intact, and no contamination was detected on the lens surface after the adhesion test. The pull-off force, which is defined as the maximum adhesion force measured during an unloading process, was measured from each sample. A contact load of 300 mN yielded a distribution of pull-off force values centered at 37.4 mN for the ZnO/G film and at 44.7 mN for the ZnO/QD/G film (Figure 3e). The improvement in the pull-off force (19.5% improvement) obtained from ZnO/QD/G indicated the role of the CdSe QDs in the bonding interaction between the graphene and the ZnO layer.

We examined the electrical properties of the contact between the ZnO and QD/G using a transmission line model.[29] The contact resistance measurements were collected on a system prepared as follows. Two electrodes separated by a channel spacing of between 10 and 70 μm were patterned by conventional photolithography combined with an oxygen

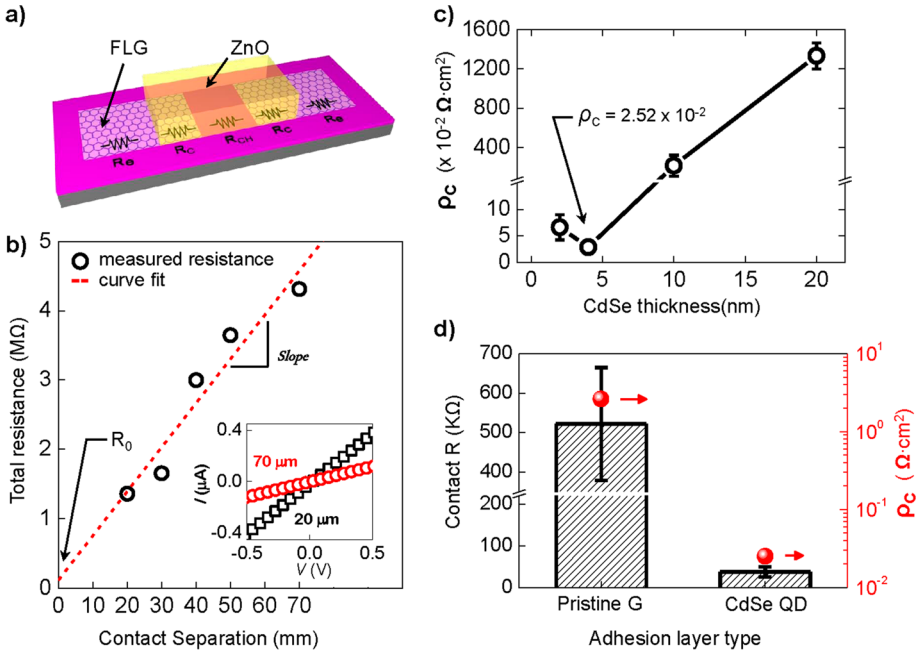

Figure 4. Contact resistance measurement between ZnO film and graphene electrode: (a) schematic drawing of the device, (b) total resistance as a function of the channel length, (c) contact resistivity of ZnO/QD/G devices as a function of QD thickness and $I-V$ plots of two devices with different channel lengths (inset), and (d) contact resistance and resistivity data on ZnO/G and ZnO/QD/G devices.

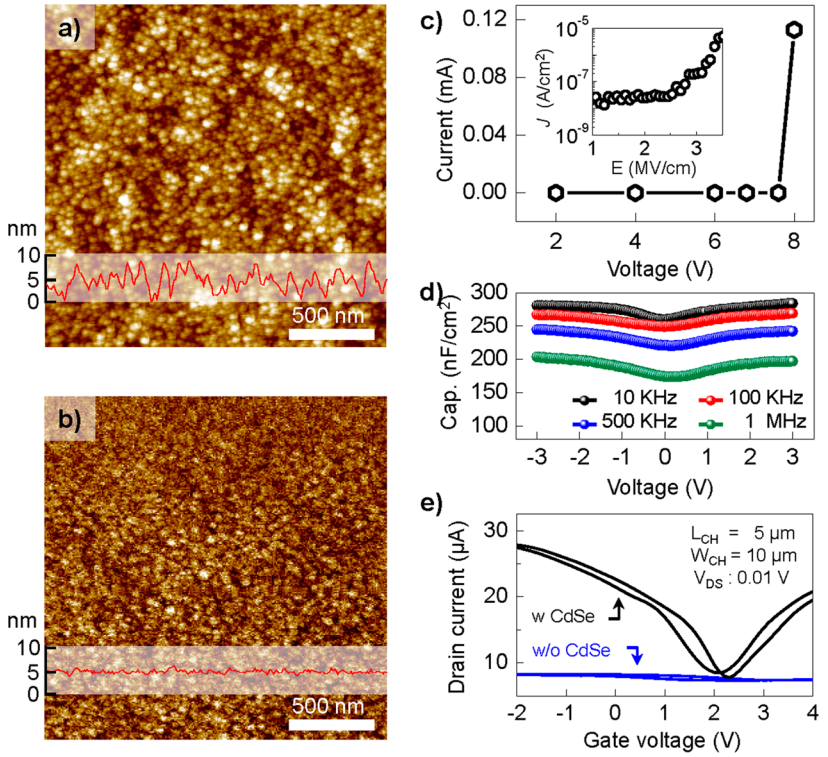

Figure 5. Characteristic of the CdSe QD-seeded HfO_2 layer prepared on CVD graphene. Topological properties of the (a) QD/G and (b) HfO_2/QD/G devices. (the height of the white box in the line profile was 10 nm) (c and d) Capacitance–voltage curve as a function of the frequency. (e) Typical transfer characteristics of HfO_2 gated graphene FET with (black) and without (blue) CdSe QDs.

plasma etching process. A 100 nm thick ZnO thin film was then sputtered over the two electrodes (Figure 4a). The resistance decreased linearly as the channel length (L_{ch}) decreased, indicating an Ohmic contact between the ZnO film and the QD/G electrodes (Figure 4b). These characteristics were distinct from the contact characteristics typical of ZnO on a pristine G layer.[30] The measured total resistance (R_{tot}) after correcting for the graphene-Au tip contact resistance (Supporting Information Figure S6) could be expressed as the sum of the internal resistance of two graphene electrodes ($2R_e$), the contact resistance ($2R_c$), and the resistance of the ZnO channel (R_{ch}), $R_{tot} = 2R_e + 2R_c + R_{ch}$. The net value of R_o

dx.doi.org/10.1021/am502922w | ACS Appl. Mater. Interfaces 2014, 6, 13015−13022

$= 2(R_e + R_c)$ could be determined based on a linear fit of the $R_{tot}-L_{ch}$ plot in Figure 4b. By subtracting R_e from R_o, the contact resistance (R_c) and the contact resistivity (ρ_c) could be calculated. Figure 4c shows the variations in ρ_c as a function of the CdSe QD thickness. For 4 nm thick QDs, ρ_c showed the minimum of 2.52×10^{-2} Ω·cm^2, a value considerably lower than that obtained from that of ZnO/G (Figure 4d). The improved electrical properties of the contact are attributed to the formation of a good interfacial binding and band alignment between the ZnO film and the graphene substrate through the help of the CdSe QD array (Supporting Information Figure S7).[32] The contact resistance data in our work can be explained in terms of "convergence and divergence of current flow" and "barrier height lowering". The concept of convergence and divergence current flow applies when the interfacial junction is nonuniform as in the ZnO-graphene interface of ZnO/G.[31,33−35] The current flow is restricted in regions where ZnO is chemically bonded to the graphene substrate, which are the defects and grain boundaries of graphene. Because the area of such regions is much smaller than the entire interface, the contact resistance is very high (Supporting Information Figure S8a). On the other hand, the introduction of CdSe QD array can provide easier and uniform paths to current flow through the improvements on the interface. Moreover, the barrier height between graphene and CdSe QDs can be lowered by thermionic-field emission when a bias is applied on the ZnO-graphene junction. Small curvature at interface of QDs nanostructure could lead to a significant incensement of electric field, which induces stronger tunneling current. As a result, the barrier height can be reduced.[36,37] Thus, the electrical and physical contact property between ZnO and graphene can be improved by introducing the CdSe QDs.

Since it is important to find out the suitable thickness of QDs to optimize the contact property, the effect of the thickness of the CdSe QDs was investigated by using QD/G with various QD thicknesses for the fabrication of ZnO/QD/G devices. ρ_c tended to increase with the thickness of the QDs (Figure 4c) due to the large resistance of the CdSe QDs (Supporting Information Figure S8b−d and S10). However, when the QD array is thinner than 4 nm, the contact resistance increases. This is probably because the graphene surface is not fully covered. In the SEM images, the 2 nm thick QD/G film (Supporting Information Figure S9) shows some regions in which uncovered graphene surface is exposed, whereas the 4 nm thick QD/G film shows full coverage of the surface with QDs. Because the nucleation and growth of CdSe QDs is a stochastic process, incomplete surface coverage is unavoidable when the layer is very thin.

In general, it is difficult to form a uniform high-k dielectric layer on graphene via ALD processes because graphene surface is hydrophobic. Additional processes, such as ozone treatment or the introduction of an organic layer, are usually applied to facilitate the initial reactions between the precursor gases and the graphene surface.[38−41] These methods tend to cause problems. For example, they degrade the electrical properties of graphene and reduce the effective capacitance of the dielectric layer. As an alternative approach, we have applied a CdSe QD array to form a uniform large-scale HfO_2 high-k dielectric film on CVD-grown graphene. Figure 5a and b show atomic force microscopy (AFM) images before and after the formation of HfO_2 ($t \sim 20$ nm) on the QD/G substrate. The images reveal a uniform HfO_2 film on the QD/G surface. The initial QD/G surfaces were characterized by a 3 nm RMS roughness due to CdSe QDs and this roughness was reduced to 1 nm after the deposition of HfO_2. This surface smoothing is because the ligand exchange probability varies depending on the surface curvature of the substrate (Supporting Information Figure S11).[42,43] Furthermore, we fabricated a metal-oxide-graphene capacitor to evaluate the dielectric properties of the high-quality HfO_2 film on QD/G. The leakage current and dielectric breakdown electric field of HfO_2 was measured first (Figure 5c). Beyond 2.5 MV/cm, the gate dielectrics began to undergo a soft breakdown. This type of breakdown often results from a weak localized percolation path between the graphene electrodes.[44] As the bias increased, the current increased dramatically due to the gate leakage. The hard breakdown field and leakage current densities of the HfO_2 film were found to be 3.8 MV/cm and 2.64×10^{-8} A/cm^2 at 2 MV/cm, respectively (inset of Figure 5c). The frequency dependence of the capacitance was measured over the range from 10 kHz to 1 MHz (Figure 5d). The normalized total capacitance values displayed a slight curvature near the zero voltage due to the quantized capacitance of graphene, which should be modeled as a one- or two-dimensional system[45] and tended to decrease as the frequency increased. The capacitance was extracted from dual-frequency measurement technique ($C \sim 270$ nF/cm^2).[46]

A feasible application was demonstrated by constructing a top-gated graphene field effect transistor (FET) based on HfO_2/QD/G. Figure 5e displays the representative transfer characteristics of top gated graphene FET with and without CdSe QD array at $V_{DS} = 0.01$ V. Even though HfO_2 dielectric layer deposited from the same batch, the HfO_2/QD/G transistor exhibited effective charge modulation according to gate voltage over that of HfO_2/G transistor (Supporting Information Figure S12). These results prove that the capacitance of HfO_2 was significantly enhanced when the CdSe QD array was introduced. Interestingly, unlike typical graphene FETs on a SiO_2 substrate, which predominantly displayed p-type ambipolar behavior, graphene FET based on HfO_2/QD/G showed enhanced n-type properties. The n-doping of carbon materials by CdSe QDs has been well documented on CdSe QD/CNT systems.[25,47] Similarly, in the present work, the CdSe QDs could donate electrons to the graphene active layer and compensate for the effects of the silanol groups on the SiO_2 substrate, as verified by the red shift in the Raman spectra and transfer characteristic. The effects of CdSe QDs on single-layer graphene were also in good agreement with the results on trilayer graphene as shown in Supporting Information (Figure S13). In addition, the narrow hysteresis of the transfer characteristic indicates the presence of a small amount of charge traps at the interface between graphene and dielectric.[48] The calculated field-effect hole and electron mobilities were 2600 and 2000 cm^2/V·s, respectively, which are comparable with previously reported ones (Supporting Information Figure S14 and Table S3).

CONCLUSION

In summary, we demonstrated an effective method for growing oxide semiconductor (i.e., ZnO) or high-k dielectric (i.e., HfO_2) films on graphene using a CdSe QD array which has intermediate bond properties between the sharply dissimilar materials. The CdSe QD array enables strong adhesion to and, thereby, uniform growth on graphene of the oxide films. The ZnO film on QD/G, grown by RF magnetron sputtering, displayed a strong adhesion force of 44.7 mN and a low contact resistance of 2.52×10^{-2} Ω·cm^2. We also fabricated a high-

speed graphene-FET based on the high-k HfO_2 dielectric. As with the ZnO film, the CdSe QD improved the bond strength between the HfO_2 and graphene layers. The hole and electron mobilities of the resultant device were 2600 and 2000 $cm^2/V{\cdot}s$, respectively. Thus, the fabrication of the proposed CdSe QD array on graphene represents a new route to the preparation of graphene-based device applications. These findings may lead to high performance devices based on graphene when applied to other functional electronic oxide materials such as indium zinc gallium oxide. Such attempts may be able to pave a new avenue toward flexible electronics in the future.

■ ASSOCIATED CONTENT

Ⓢ Supporting Information

Raman spectra and contact angles of trilayer graphene with and without CdSe QDs, XPS depth profiles of O 1s and Zn 2p regions, illustration of adhesion test, total contact resistance, energy band diagrams of ZnO/graphene heterojunction, illustration of current flow path, SEM images of CdSe QDs/graphene, current−voltage characteristic of ZnO/graphene junction, illustration of nucleation process of ALD, representative ID-VG characteristic of top gate G-FET, Optical transmittance spectra of single-layer graphene (SLG) on the PET and the Raman spectrum on SiO2/Si substrate, transistor character with and without CdSe QDs, conductivity vs carrier density plot of G-FET using HfO_2, parameter of adhesion test, XPS peak analyses of the Cd 3d and Se 3d regions, comparison of top-gate graphene transistor properties. This material is available free of charge via the Internet at http://pubs.acs.org.

■ AUTHOR INFORMATION

Corresponding Authors

*Fax: +82 31 299 4179. Tel: +82 31 290 7070. E-mail: ywkwon@skku.edu (Y.-U.K.).
*E-mail: ahnj@yonsei.ac.kr (J.-H.A.).

Author Contributions

‖Y.-T.K. and S.-K.L. contributed equally to this work.

Funding

This work was supported by the National Research Foundation of Korea (NRF) grants funded by the Korean Government (20090081018, 20090094023, 20090083540, 2012R1A2A1A03006049, and 2013R1A1A2065629).

Notes

The authors declare no competing financial interest.

■ REFERENCES

(1) Chung, K.; Lee, C. H.; Yi, G. C. Transferable GaN Layers Grown on ZnO-Coated Graphene Layers for Optoelectronic Devices. *Science* **2010**, *330*, 655−657.

(2) Lee, C. H.; Kim, Y. J.; Hong, Y. J.; Jeon, S. R.; Bae, S.; Hong, B. H.; Yi, G. C. Flexible Inorganic Nanostructure Light-Emitting Diodes Fabricated on Graphene Films. *Adv. Mater.* **2011**, *23*, 4614−4619.

(3) Chang, C.-W.; Tan, W.-C.; Lu, M.-L.; Pan, T.-C.; Yang, Y.-J.; Chen, Y.-F. Graphene/SiO2/p-GaN Diodes: An Advanced Economical Alternative for Electrically Tunable Light Emitters. *Adv. Funct. Mater.* **2013**, *23*, 4043−4048.

(4) Yan, Z.; Liu, G.; Khan, J. M.; Balandin, A. A. Graphene Quilts for Thermal Management of High-Power GaN Transistors. *Nat. Commun.* **2012**, *3*, 827.

(5) Eda, G.; Fanchini, G.; Chhowalla, M. Large-Area Ultrathin Films of Reduced Graphene Oxide as a Transparent and Flexible Electronic Material. *Nat. Nanotechnol.* **2008**, *3*, 270−274.

(6) Yu, W. J.; Lee, S. Y.; Chae, S. H.; Perello, D.; Han, G. H.; Yun, M.; Lee, Y. H. Small Hysteresis Nanocarbon-Based Integrated Circuits on Flexible and Transparent Plastic Substrate. *Nano Lett.* **2011**, *11*, 1344−1350.

(7) Wu, J.; Becerril, H. A.; Bao, Z.; Liu, Z.; Chen, Y.; Peumans, P. Organic Solar Cells with Solution-Processed Graphene Transparent Electrodes. *Appl. Phys. Lett.* **2008**, *92*, 263302.

(8) Park, H.; Brown, P. R.; Bulović, V.; Kong, J. Graphene As Transparent Conducting Electrodes in Organic Photovoltaics: Studies in Graphene Morphology, Hole Transporting Layers, and Counter Electrodes. *Nano Lett.* **2011**, *12*, 133−140.

(9) Gomez De Arco, L.; Zhang, Y.; Schlenker, C. W.; Ryu, K.; Thompson, M. E.; Zhou, C. Continuous, Highly Flexible, and Transparent Graphene Films by Chemical Vapor Deposition for Organic Photovoltaics. *ACS Nano* **2010**, *4*, 2865−2873.

(10) Wang, X.; Zhi, L.; Müllen, K. Transparent, Conductive Graphene Electrodes for Dye-Sensitized Solar Cells. *Nano Lett.* **2007**, *8*, 323−327.

(11) Kavan, L.; Yum, J. H.; Grätzel, M. Optically Transparent Cathode for Dye-Sensitized Solar Cells Based on Graphene Nanoplatelets. *ACS Nano* **2010**, *5*, 165−172.

(12) Velten, J. A.; Carretero-González, J.; Castillo-Martínez, E.; Bykova, J.; Cook, A.; Baughman, R.; Zakhidov, A. Photoinduced Optical Transparency in Dye-Sensitized Solar Cells Containing Graphene Nanoribbons. *J. Phys. Chem. C* **2011**, *115*, 25125−25131.

(13) Lee, S.; Jo, G.; Kang, S. J.; Wang, G.; Choe, M.; Park, W.; Kim, D. Y.; Kahng, Y. H.; Lee, T. Enhanced Charge Injection in Pentacene Field-Effect Transistors with Graphene Electrodes. *Adv. Mater.* **2011**, *23*, 100−105.

(14) Han, T.-H.; Lee, Y.; Choi, M.-R.; Woo, S.-H.; Bae, S.-H.; Hong, B. H.; Ahn, J.-H.; Lee, T.-W. Extremely Efficient Flexible Organic Light-Emitting Diodes with Modified Graphene Anode. *Nat. Photonics* **2012**, *6*, 105−110.

(15) Wang, Y.; Tong, S. W.; Xu, X. F.; Ozyilmaz, B.; Loh, K. P. Interface Engineering of Layer-by-Layer Stacked Graphene Anodes for High-Performance Organic Solar Cells. *Adv. Mater.* **2011**, *23*, 1514−1518.

(16) Guo, C. X.; Yang, H. B.; Sheng, Z. M.; Lu, Z. S.; Song, Q. L.; Li, C. M. Layered Graphene/Quantum Dots for Photovoltaic Devices. *Angew. Chem., Int. Ed.* **2010**, *49*, 3014−3017.

(17) Lightcap, I. V.; Kamat, P. V. Fortification of CdSe Quantum Dots with Graphene Oxide. Excited State Interactions and Light Energy Conversion. *J. Am. Chem. Soc.* **2012**, *134*, 7109−7116.

(18) Jandhyala, S.; Mordi, G.; Lee, B.; Lee, G.; Floresca, C.; Cha, P.-R.; Ahn, J.; Wallace, R. M.; Chabal, Y. J.; Kim, M. J.; Colombo, L.; Cho, K.; Kim, J. Atomic Layer Deposition of Dielectrics on Graphene Using Reversibly Physisorbed Ozone. *ACS Nano* **2012**, *6*, 2722−2730.

(19) Sangwan, V. K.; Jariwala, D.; Filippone, S. A.; Karmel, H. J.; Johns, J. E.; Alaboson, J. M.; Marks, T. J.; Lauhon, L. J.; Hersam, M. C. Quantitatively Enhanced Reliability and Uniformity of High-Kappa Dielectrics on Graphene Enabled by Self-Assembled Seeding Layers. *Nano Lett.* **2013**, *13*, 1162−1167.

(20) Wang, Z.; Xu, H.; Zhang, Z.; Wang, S.; Ding, L.; Zeng, Q.; Yang, L.; Pei, T.; Liang, X.; Gao, M.; Peng, L. M. Growth and Performance of Yttrium Oxide as an Ideal High-Kappa Gate Dielectric for Carbon-Based Electronics. *Nano Lett.* **2010**, *10*, 2024−2030.

(21) Wang, L.; Chen, X.; Wang, Y.; Wu, Z.; Li, W.; Han, Y.; Zhang, M.; He, Y.; Zhu, C.; Fung, K. K.; Wang, N. Modification of Electronic Properties of Top-Gated Graphene Devices by Ultrathin Yttrium-Oxide Dielectric Layers. *Nanoscale* **2013**, *5*, 1116−1120.

(22) Kim, Y.-T.; Han, J. H.; Hong, B. H.; Kwon, Y.-U. Electrochemical Synthesis of CdSe Quantum-Dot Arrays on a Graphene Basal Plane Using Mesoporous Silica Thin-Film Templates. *Adv. Mater.* **2010**, *22*, 515−518.

(23) Kim, Y.-T.; Shin, H.-W.; Ko, Y.-S.; Ahn, T. K.; Kwon, Y.-U. Synthesis of a CdSe-Graphene Hybrid Composed of CdSe Quantum Dot Arrays Directly Grown on CVD-Graphene and its Ultrafast Carrier Dynamics. *Nanoscale* **2013**, *5*, 1483−1488.

(24) Li, X.; Cai, W.; An, J.; Kim, S.; Nah, J.; Yang, D.; Piner, R.; Velamakanni, A.; Jung, I.; Tutuc, E.; Banerjee, S. K.; Colombo, L.;

Ruoff, R. S. Large-Area Synthesis of High-Quality and Uniform Graphene Films on Copper Foils. *Science* **2009**, *324*, 1312−1314.
(25) Lee, U.-H.; Yang, J.-H.; Lee, H.-J.; Park, J.-Y.; Lee, K.-R.; Kwon, Y.-U. Facile and Adaptable Synthesis Method of Mesostructured Silica Thin Films. *J. Mater. Chem.* **2008**, *112*, 8419−8423.
(26) Koh, J. L.; Teh, L. K.; Romanato, F.; Wong, C. C. Temperature Dependence of Electrochemical Deposition of CdSe. *J. Electrochem.* **2007**, *154*, D300−D303.
(27) Juárez, B. H.; Klinke, C.; Kornowski, A.; Weller, H. Quantum Dot Attachment and Morphology Control by Carbon Nanotubes. *Nano Lett.* **2007**, *7*, 3564−3568.
(28) Hungría, A.; Juárez, B.; Klinke, C.; Weller, H.; Midgley, P. 3-D Characterization of CdSe Nanoparticles Attached to Carbon Nanotubes. *Nano Res.* **2008**, *1*, 89−97.
(29) Hertel, S.; Waldmann, D.; Jobst, J.; Albert, A.; Albrecht, M.; Reshanov, S.; Schoner, A.; Krieger, M.; Weber, H. B. Tailoring the Graphene/Silicon Carbide Interface for Monolithic Wafer-Scale Electronics. *Nat. Commun.* **2012**, *3*, 957.
(30) Kim, S.; Janes, D. B.; Choi, S.-Y.; Ju, S. Nanoscale Contacts Between Semiconducting Nanowires and Metallic Graphenes. *Appl. Phys. Lett.* **2012**, *101*, 063122.
(31) Carlson, B.; Leschkies, K.; Aydil, E. S.; Zhu, X. Y. Valence Band Alignment at Cadmium Selenide Quantum Dot and Zinc Oxide (1010) Interfaces. *J. Phys. Chem. C* **2008**, *112*, 8419−8423.
(32) Wilson, W. E.; Angadi, S. V.; Jackson, R. L. Surface Separation and Contact Resistance Considering Sinusoidal Elastic-Plastic Multi-Scale Rough Surface Contact. *Wear* **2010**, *268*, 190−201.
(33) Kogut, L.; Komvopoulos, K. Electrical Contact Resistance Theory for Conductive Rough Surfaces Separated by a Thin Insulating Film. *J. Appl. Phys.* **2004**, *95*, 576−585.
(34) Duong, D. L.; Han, G. H.; Lee, S. M.; Gunes, F.; Kim, E. S.; Kim, S. T.; Kim, H.; Ta, Q. H.; So, K. P.; Yoon, S. J.; Chae, S. J.; Jo, Y. W.; Park, M. H.; Chae, S. H.; Lim, S. C.; Choi, J. Y.; Lee, Y. H. Probing Graphene Grain Boundaries with Optical Microscopy. *Nature* **2012**, *490*, 235−240.
(35) Tsen, A. W.; Brown, L.; Levendorf, M. P.; Ghahari, F.; Huang, P. Y.; Havener, R. W.; Ruiz-Vargas, C. S.; Muller, D. A.; Kim, P.; Park, J. Tailoring Electrical Transport Across Grain Boundaries in Polycrystalline Graphene. *Science* **2012**, *336*, 1143−1146.
(36) Yang, W.; Jedema, F. J.; Ade, H.; Nemanich, R. J. Correlation of Morphology and Electrical Properties of Nanoscale TiSi2 Epitaxial Islands on Si (001). *Thin Solid Films* **1997**, *308*, 627−633.
(37) Jiang, Y.-L.; Qu, X.-P.; Ru, G.-P.; Li, B.-Z. Schottky Barrier Height Lowering Induced by CoSi2 Nanostructure. *Appl. Phys. A: Mater. Sci. Process.* **2010**, *99*, 93−98.
(38) Williams, J. R.; DiCarlo, L.; Marcus, C. M. Quantum Hall Effect in a Gate-Controlled p-n Junction of Graphene. *Science* **2007**, *317*, 638−641.
(39) Lee, B.; Mordi, G.; Kim, M. J.; Chabal, Y. J.; Vogel, E. M.; Wallace, R. M.; Cho, K. J.; Colombo, L.; Kim, J. Characteristics of High-k Al2O3 Dielectric using Ozone-Based Atomic Layer Deposition for Dual-Gated Graphene Devices. *Appl. Phys. Lett.* **2010**, *97*, 043107.
(40) Fallahazad, B.; Lee, K.; Lian, G.; Kim, S.; Corbet, C. M.; Ferrer, D. A.; Colombo, L.; Tutuc, E. Scaling of Al2O3 Dielectric for Graphene Field-Effect Transistors. *Appl. Phys. Lett.* **2012**, *100*, 093112.
(41) Meric, I.; Dean, C. R.; Young, A. F.; Baklitskaya, N.; Tremblay, N. J.; Nuckolls, C.; Kim, P.; Shepard, K. L. Channel Length Scaling in Graphene Field-Effect Transistors Studied with Pulsed Current-Voltage Measurements. *Nano Lett.* **2011**, *11*, 1093−1097.
(42) Alam, M. A.; Green, M. L. Mathematical Description of Atomic Layer Deposition and its Application to the Nucleation and Growth of HfO_2 Gate Dielectric Layers. *J. Appl. Phys.* **2003**, *94*, 3403−3413.
(43) Szeghalmi, A.; Helgert, M.; Brunner, R.; Heyroth, F.; Gosele, U.; Knez, M. Tunable Guided-Mode Resonance Grating Filter. *Adv. Funct. Mater.* **2010**, *20*, 2053−2062.
(44) Nigam, T.; Degraeve, R.; Groeseneken, G.; Heyns, M. M.; Maes, H. E. In Constant current charge-to-breakdown: Still a valid tool to study the reliability of MOS structures? *36th Annual IEEE International Reliability Physics Symposium Proceedings*, Reno, NV, March 31−April 2 1998; pp 62−69.
(45) Xia, J. L.; Chen, F.; Li, J. H.; Tao, N. J. Measurement of the Quantum Capacitance of Graphene. *Nat. Nanotechnol.* **2009**, *4*, 505−509.
(46) Alaboson, J. M. P.; Wang, Q. H.; Emery, J. D.; Lipson, A. L.; Bedzyk, M. J.; Elam, J. W.; Pellin, M. J.; Hersam, M. C. Seeding Atomic Layer Deposition of High-k Dielectrics on Epitaxial Graphene with Organic Self-Assembled Monolayers. *ACS Nano* **2011**, *5*, 5223−5232.
(47) Nath, M.; Teredesai, P. V.; Muthu, D. V. S.; Sood, A. K.; Rao, C. N. R. Single-Walled Carbon Nanotube Bundles Intercalated with Semiconductor Nanoparticles. *Curr. Sci.* **2003**, *85*, 956−960.
(48) Shin, W. C.; Seo, S.; Cho, B. J. Highly Air-Stable Electrical Performance of Graphene Field Effect Transistors by Interface Engineering with Amorphous Fluoropolymer. *Appl. Phys. Lett.* **2011**, *98*, 153505.